Observation of dispersive shock waves developing from initial depressions in shallow water

Article *in* Physica D Nonlinear Phenomena · January 2016

DOI: 10.1016/j.physd.2016.01.007

CITATIONS
42

READS
206

4 authors, including:

Stefano Trillo
University of Ferrara
433 PUBLICATIONS **10,080** CITATIONS
SEE PROFILE

Marco Klein
Technische Universität Hamburg
45 PUBLICATIONS **494** CITATIONS
SEE PROFILE

Miguel Onorato
Università degli Studi di Torino
238 PUBLICATIONS **8,317** CITATIONS
SEE PROFILE

Accepted Manuscript

Observation of dispersive shock waves developing from initial depressions in shallow water

S. Trillo, M. Klein, G. Clauss, M. Onorato

PII: S0167-2789(16)00007-5
DOI: http://dx.doi.org/10.1016/j.physd.2016.01.007
Reference: PHYSD 31740

To appear in: *Physica D*

Received date: 30 September 2015
Revised date: 12 January 2016
Accepted date: 14 January 2016

Please cite this article as: S. Trillo, M. Klein, G. Clauss, M. Onorato, Observation of dispersive shock waves developing from initial depressions in shallow water, *Physica D* (2016), http://dx.doi.org/10.1016/j.physd.2016.01.007

S. Trillo et al.
Observation of dispersive shock waves developing from initial depressions in shallow water, submitted to Physica D (special issue dispersive hydrodynamics)

Highlights

- We observe dispersive shock waves in a shallow water tank
- Different levels of nonlinearity and dispersion are contrasted
- Data are compared with numerics based on the Korteweg-deVries and Whitham equations

Available online at www.sciencedirect.com

ScienceDirect

Physica D

ELSEVIER

Physica D 00 (2016) 1–9

Observation of dispersive shock waves developing from initial depressions in shallow water

S. Trillo[a], M. Klein[b], G. Clauss[b], M. Onorato[c,d]

[a]*Department of Engineering, University of Ferrara, Via Saragat 1, 44122 Ferrara, Italy*
[b]*Technical University of Berlin, Ocean Engineering Division, Sekr. SG-17, Salzufer 17-19,10587 Berlin, Germany*
[c]*Dipartimento di Fisica Generale, Università di Torino, Via P. Giuria, 1, 10125 Torino, Italy*
[d]*Istituto Nazionale di Fisica Nucleare, INFN, Sezione di Torino, 10125 Torino, Italy*

Abstract

We investigate surface gravity waves in a shallow water tank, in the limit of long wavelengths. We report the observation of non-stationary dispersive shock waves rapidly expanding over a 90 m flume. They are excited by means of a wave maker that allows us to launch a controlled smooth (single well) depression with respect to the unperturbed surface of the still water, a case that contains no solitons. The dynamics of the shock waves are observed at different levels of nonlinearity equivalent to a different relative smallness of the dispersive effect. The observed undulatory behaviour is found to be in good agreement with the dynamics described in terms of a Korteweg-de Vries equation with evolution in space, though in the most nonlinear cases the description turns out to be improved over the quasi linear trailing edge of the shock by modelling the evolution in terms of the integro-differential (nonlocal) Whitham equation.

Keywords: Water waves, Dispersive shock waves, Korteweg-de Vries equation, Whitham equation

1. Introduction

Dispersive shock waves (DSWs) are non-stationary wave trains that form spontaneously in weakly dispersive media [1]. The underlying mechanism is the wave steepening driven by the nonlinearity which leads to a gradient catastrophe, regularized by dispersion that becomes important close to the point where strong gradients are formed. Usually, the oscillations expand in a so-called shock fan characterized by a leading edge and a trailing edge, where the amplitude of the oscillations are largest and vanishingly small, respectively. DSWs constitute the dispersive counterpart of the viscous regularization of classical shock waves [2]; in the latter the dissipation dominates over dispersive effects.

Pioneering works on DSWs appeared between the 60's and the 70's. Sagdeev and coworkers predicted the oscillatory nature of the shock occurring in the extremely rarefied (collisionless) plasma [3]. The observation of such dispersive breaking in the lab was reported as early as 1970 [4]. In a seminal paper for the whole area of nonlinear waves, Zabuski and Kruskal [5] numerically investigated the evolution of a sine wave according to the weakly dispersive Korteweg-de Vries (KdV) equation [6, 7, 8], finding that the gradient catastrophe of the original waveform gives rise to oscillations which evolve into secondary waves with soliton features, eventually exhibiting recurrence of the input state after collisions [5]. Strictly speaking the wave packets emerging from the breaking of the periodic waves are multiple finite-gap solutions [9] which, however, resemble solitons, especially in the limit of weak dispersion where the Floquet bands dramatically shrink. However, DSWs can form also for initial conditions which possess no soliton content. A milestone towards a more general description was the solution of the Riemann problem (the evolution of a step initial datum) for the KdV, reported by Gurevich and Pitaeviskii [10], who proposed the first explicit construction of the DSW by exploiting Whitham modulation theory [11]. The description of dispersive shocks still constitutes nowadays one of the most prolific application of such general averaging method proposed by Whitham. The KdV has also played a pivotal role for the formulation of the limit of vanishing dispersion in the framework of the inverse scattering theory [12, 13, 14, 15, 16]. In particular the case of initial data with non-soliton content was addressed in [17, 18]. Note that this limit is highly non-trivial since, at variance with the limit of vanishing viscosity, in dispersive settings

Email addresses: stefano.trillo@unife.it (S. Trillo), klein@naoe.tu-berlin.de (M. Klein), miguel.onorato@gmail.com (M. Onorato)

it never leads to the classical (dispersionless) shock wave, since the oscillations become shorter and denser as the dispersion get weaker. Nowadays the KdV still remain a very important equation as it allows for testing more accurate asymptotic descriptions of the oscillatory zone [19, 20, 21]. However, it was realized since the beginning that DSWs constitute an ubiquitous behaviour in several other dispersive Hamiltonian systems [22, 23, 24, 25]. A remarkable universal example is the nonlinear Schrödinger (NLS) equation. In this context, experimental results on DSWs have been recently reported in the field of Bose-Einstein condensed atoms [26, 27, 28, 29, 30, 31] and nonlinear optics [32, 33, 34, 35, 36, 37, 38, 39]. Such experiments have also contributed to clearly highlight the contrast associated with solitonic-type of DSWs [26, 36, 39] (see also [40, 41, 42, 43] for theoretical aspects), and nonsoliton DSWs [e.g., [27, 32, 33, 34]]. It should be noted that DSWs are also observed in nonintegrable systems, for which modulation equations can be still introduced, see for example [44].

In the context of water waves, DSWs (we stick to the term DSW for interdisciplinary purpose, though in the literature in this area, the term "undular bore" is more usually encountered) have also a long dating history. Important theoretical contributions came from Benjamin and Lighthill [45], Peregrine (who employed a model known as Benjamin-Bona-Mahony (BBM) equation [46]), and Johnson (who also investigated the effect of viscosity by means of a KdV-Burger model [47]). The most common situation is that of a bore moving into still water; for moderate amplitudes, it gives rise to undular behavior while, for larger amplitudes, undulations are still observed but the first wave is breaking. In the strongly nonlinear regime, no undulations are observed and a turbulent breaking front propagates. These phenomena can be observed in nature, with spectacular manifestations involving tidal bores in river estuaries (e.g., the Dordogne river in France, the Severn river in Wales, the Qiantang river in China, etc.), where the undular bores are also known under different local names [48].

Apparently, the laboratory investigations of undular bores was pioneered by Favre as early as 1935 [49]. Indeed, the secondary waves produced by the steep bore are also termed in hydraulic applications as Favre waves [50, 51]. However, it is again in the seventies that laboratory experiments performed in shallow water with long waves have been reported and interpreted in terms of KdV dynamics [52, 53, 54, 55, 56, 57]. Later review of such experiments have also pointed out the importance that the dynamics of the generated wavetrains can have in the interpretation of seismic generated tsunamis [58]. However, those experiments mainly dealt with initially positive elevations above the water surface, which produce multiple solitons. Only occasional observations were reported for smooth depressions, a case which cannot be interpreted in terms of generated solitons [53, 55, 56]. Moreover, such measurements suffered from limitations arising from the length of the wave-tank and by the technique used to launch the waves, employing a vertically moving piston. In this paper, we show that very extended and clean DSWs can be excited in a long tank (90 m) by using a wave maker which allows for a good degree of accuracy over the initial shape. In particular, we focus on initial depressions with profile close to square hyperbolic secant. In the initial stage where dispersion plays a negligible role, the wave evolves according to the Hopf (or inviscid Burger) equation, and experiences rarefaction on one edge and steepening over the opposite edge. The DSW that emerges from the steepened front, must be interpreted, in this case, as a genuine modulated nonlinear periodic function which is spontaneously generated due to the action of dispersion. We characterize the expansion of such DSW, comparing with numerical simulations based on a suitable form of the KdV equation and its extension introduced by Whitham. The regime that we investigate allows for observing a quite regular and extended oscillatory zone. Conversely, the length of the tank precludes the possibility to investigate the long-term asymptotic where one could expect major differences with the case of solitonic DSW (in the latter case, several solitons would asymptotically separate, as it would be the case for a positive square hyperbolic secant of proper amplitude). The characterisation of the mid-term DSW developing from the depression is also useful in view of further studies devoted to study the interaction of genuine solitons and DSWs which can occur for more general initial shapes.

The paper is organised as follows. In Sec. 2 we present the asymptotic models that we employ in order to describe the experiment, emphasising that such models are written in such a way to evolve time series in space. In Sec. 3 we present the experimentally observed data, and in Sec. 4 we discuss the numerical modelling of our observations. Finally, we summarize our finding in Sec. 5.

2. The Korteweg-de Vries equation and the Whitham equation in their spatial evolution form

The fully nonlinear viscous equations that describe the evolution of surface gravity waves are definitely too much complicated (even from a numerical treatment) to understand basic mechanisms such as solitons, breathers or DSWs. Therefore, approximations are needed if one is interested in capturing some specific nonlinear wave dynamics. Indeed, Bouissinesq [7] and Korteweg and de Vries [6] made use of asymptotic methods for deriving what is now known as the KdV equation (for discussion on the differences between the methods used in the derivation see [8]). The motivation of their work was the physical explanation of the observation of the "Wave of Translation" made by Scott Russell in 1834.

The classical derivation of the KdV equation (see for example [2]) from the Navier-Stokes equations requires a number of hypotheses: the fluid is considered inviscid and the flow irrotational; waves have long wavelength and propagation in only one direction is allowed. The key point in the derivation is the introduction of two nondimensional parameters: the first one is the nonlinear parameter, $\alpha = \eta_0/h$, where η_0 is a characteristic wave amplitude and h is the unperturbed water depth; the second one is the dispersive or the shallow water parameter, $\beta = kh$, with k a characteristic wave number of the problem under examination. "Waves of Translations" with a permanent form are the result of a balance between nonlinearity and dispersion, therefore the KdV equation is obtained by balancing α

and β. Note that if one expands the unidirectional dispersion relation for water waves, $\omega(k) = \sqrt{gk\tanh(kh)}$, in powers of kh, i.e. in the shallow water limit, at the leading order the dynamics turns out to be nondispersive, $\omega = \sqrt{gh}\,k$; therefore, if one is interested in balancing nonlinearity and dispersion, then one should choose $\alpha \sim \beta^2$. This is the fundamental assumption for the derivation of the KdV equation.

In dimensional variables the KdV equation takes the following form:

$$\eta_t + c_0\eta_z + \frac{3}{2}\frac{c_0}{h}\eta\eta_z + \frac{1}{6}c_0h^2\eta_{zzz} = 0 \tag{2.1}$$

where $c_0 = \sqrt{gh}$ is the phase velocity of linear waves and z the propagation coordinate. When dealing with experimental data in a wave tank, it is preferable to write the KdV equation as an evolution equation in space. The reason is that the wave maker produces waves that are known in time at one end of the tank and evolve along it; the boundary value problem for the original KdV equation becomes a Cauchy problem for the new equation where the evolution variable is space rather than time In this way time series measured at fixed locations along the propagation direction can be directly compared with those obtained by direct integration of the evolution model (it is interesting to note that this is analogous to what is usually done in optical fibers and described in terms of NLS equation [32, 39]). In order to derive the evolution equation in space, we consider the leading order relation in Eq. (2.1), i.e.

$$\eta_z \sim -\frac{1}{c_0}\eta_t \tag{2.2}$$

and plug it in the higher order terms to obtain the following KdV equation

$$\eta_z + \frac{1}{c_0}\eta_t - \chi\eta\eta_t - \beta_3\eta_{ttt} = 0, \tag{2.3}$$
$$\chi = \frac{3}{2}\frac{1}{c_0h}\,;\quad \beta_3 = \frac{1}{6}\frac{h^2}{c_0^3},$$

with associated initial value $\eta(z=0,t) = \eta_0 f_0(t/t_0)$, η_0 and t_0 being the initial wave amplitude and duration, respectively, and $f_0(t)$ fixing the shape with normalization such to have absolute unit maximum. Following [59, 60], the above equation will be named time-like Korteweg-de Vries (T-KdV) equation. Here we emphasize that equation (2.3) cannot be derived by an exact transformation from Eq. (2.1); however, they both have formally the same asymptotic validity. Nonetheless, a straightforward analysis, shows that the linear dispersion relation obtained from the T-KdV equation shows a better agreement with the full dispersion relation with respect to the one obtained from the KdV. Indeed, the linear dispersion for the KdV equation (2.1) turns out to be

$$D(\omega,k) = \omega - c_0k + \frac{1}{6}c_0h^2k^3 = 0, \tag{2.4}$$

whereas for the T-KdV equation (2.3), we obtain

$$D(\omega,k) = k - \frac{\omega}{c_0} - \frac{1}{6}\frac{h^2}{c_0^3}\omega^3 = 0. \tag{2.5}$$

The phase velocity $v_p = \omega/k$ normalized by c_0 for both equations as a function of kh is plotted against the one obtained from the full dispersion relation in Fig. 1. Clearly, the linear phase velocity obtained from the T-KdV equation results in a better agreement to the full dispersion relation with respect to the one from the KdV equation. For example for $kh = 0.7$ the error on the velocity from standard KdV is of the order of 1% while it is of the order of 0.04% for the T-KdV. Amazingly, for $kh = 5$, i.e. well beyond the validity of the KdV approximation, the error over the phase velocity is only of the order of 10% for the T-KdV.

The relative weight of dispersion and nonlinearity can be usefully quantified by casting Eq. (2.3) in the dimensionless form usually employed to apply asymptotic analysis of the DSW (see, e.g. Refs. [5, 10, 27, 19])

$$u_\zeta - uu_\tau - \varepsilon^2u_{\tau\tau\tau} = 0, \tag{2.6}$$
$$u(0,\tau) = f_0(\tau). \tag{2.7}$$

In Eq. (2.6) we have introduced the retarded time $\tau = (t - z/c_0)/t_0$, the distance $\zeta = z/L_{nl}$, and the normalized elevation $u = \eta/\eta_0$, where t_0 and η_0 are the duration and the elevation of the initial disturbance, respectively, and we defined $L_{nl} = t_0/(\chi\eta_0)$ as the nonlinear length, that is, the characteristic length scale after which the effects due to the nonlinearity become significant. The weakness of the dispersive effect is measured by the ratio between L_{nl} and the characteristic length scale of the dispersion, namely $L_d = t_0^3/\beta_3$, i.e. by the smallness parameter

$$\varepsilon^2 = \frac{L_{nl}}{L_d} = \frac{\beta_3}{\chi}\frac{1}{\eta_0t_0^2} = \frac{1}{9}\frac{h^3}{c_0^2}\frac{1}{\eta_0t_0^2}. \tag{2.8}$$

Such quantity can be related to the so-called Ursell number $U = \frac{\eta_0}{h}\left(\frac{\lambda}{h}\right)^2 \sim \frac{\alpha}{\beta^2}$ [61, 53], as follows

$$\varepsilon^2 = \frac{(2\pi)^2}{9}\frac{h^3}{\eta_0\lambda^2} = \frac{(2\pi)^2}{9}\frac{1}{U}. \tag{2.9}$$

In order to improve the accuracy of the description of the surface gravity waves towards short wave numbers, we also make use of the Whitham equation [62, 63]. In its original formulation Whitham proposed to improve the KdV equation (2.1) by replacing the third-order derivative with a convolution that accounts for the full unidirectional dispersion relation. Once expressed by means of the Fourier transforms, the dimensional Whitham equation has the following form:

$$\eta_t + \frac{3}{2}\frac{c_0}{h}\eta\eta_z + \mathcal{F}^{-1}\left[i\,sign(k)\omega(k)\mathcal{F}\left[\eta\right]\right] = 0, \tag{2.10}$$

where $\mathcal{F}[...]$ is the Fourier Transform operator in space. Note that the convolution is expressed here, in Fourier space, in terms of η instead of η_x as in Whitham original formulation, with a redefinition of the Kernel, which in the original formulation was the inverse tranform of the velocity $v(k) = \omega(k)/k$. The Whitham equation has been widely discussed in the literature. It has been shown that the equation admits periodic travelling-wave solutions whose stability has been studied in [64]. In

Ref. [65] it has been identified a scaling regime in which the Whitham equation can be derived from the Hamiltonian formulation of surface water waves. Numerical simulations of the Whitham equation have also been performed and compared with Euler, KdV and BBM simulations; it has been shown that in a wide parameter range of amplitudes and wavelengths, the Whitham equation performs equally or better than the KdV or the BBM equations [65]. Finally, the role of having bidirectional wave propagation was recently addressed in [66], particularly with reference to high-frequency instabilities.

With the aim of comparing our numerical simulations with experimental data in the wave tank, we find useful to write the Whitham equation as an evolution equation in space as follows:

$$\eta_z - \chi\eta\eta_t - \mathcal{F}^{-1}\left[i\, sign(\omega)k(\omega)\mathcal{F}\left[\eta\right]\right] = 0, \qquad (2.11)$$

where now $\mathcal{F}[...]$ is the Fourier Transform operator in time and $k(\omega)$ results from the inversion of the full linear dispersion relation of surface gravity waves. We will term the above equation as the time-like Whitham equation and denote it by T-Whitham. We have performed numerical simulations of Eqs. (2.3) and (2.11) and results will be compared in Section 4 with experimental data.

3. The experiment

The experiment is performed in the sea-keeping basin of the Technical University of Berlin. The basin is 110 m long, with a measuring range of $L = 90$ m. The width of the basin is 8 m and the water depth has been adjusted to $h = 0.4$ m. On the one side, an electrically driven wave generator is installed, which can be utilized in piston-type as well as flap-type mode. The control software features the generation of transient wave packages, deterministic irregular sea states with predefined characteristics as well as tailored critical wave sequences [67]. In this study, the wave generator is driven in piston-type mode which provides a horizontal particle velocity profile at the wave board close to the physical one. The hydrodynamic transfer function of the wave generator is modelled using the Biesel function [68] relating the wave board stroke to the wave amplitude at the position of the wave maker linearly. On the opposite (downstream) side, a wave damping slope (beach) is installed to limit the disturbing wave reflections. The test setup comprises eight wave gauges which are installed along the basin, starting with the first at 5 m in front of the wave generator to 75 m with a constant relative spacing of 10 m (at distances $z = 5, 15, 25, 35, 45, 55, 65, 75$ m from the wave maker at $z = 0$).

The target surface elevation in front of the wave maker was established to be nominally

$$\eta(z = 0, t) = -\eta_0 \mathrm{sech}^2\left(\frac{t}{t_0}\right), \qquad (3.1)$$

i.e. a depression reaching an amplitude of η_0 and width proportional to t_0. By employing the wave maker as a horizontally moving piston, it has not been a trivial task to generate the desired shape of the surface depression with adjustable wave amplitude, and only after some trials and errors the goal was achieved with a good degree of reliability. Therefore, for the data set reported below, we are confident that the launched wave is of the form of Eq. (3.1). To this end we also rely on the agreement between the numerical integration of the KdV with initial condition (3.1) and the experimental results (see also Section 4).

	run A	run B	run C
η_0 [cm]	2	4	10
t_0 [s]	1.27	1.27	0.64
L_d [m]	601	601	75
L_{nl} [m]	33.6	16.8	3.4
ε^2	0.056	0.028	0.045
Ursell Number	78	157	98

Table 1. Initial value parameters: wave amplitude η_0 and duration t_0 in Eq. (3.1) for the three experimental runs shown in Figs. 2-4, and corresponding values of dispersion (L_d) and nonlinear (L_{nl}) length scales, as well as dispersion smallness parameter ε^2 and the Ursell number U.

In term of the dimensionless initial value problem in Eqs. (2.6)-(2.7), Eq. (3.1) is equivalent to set $f_0(\tau) = -\mathrm{sech}^2(\tau)$. During propagation such initial condition evolves in such a way that its temporal edge with negative slope smooth out (it rarefies using the language of gas dynamics, i.e. its slope gradually decreases), whereas its positive slope edge steepen. It is worth pointing out that this is the opposite of what is usually reported for the standard KdV [5, 10, 19], due to the opposite sign of the nonlinear term in the T-KdV equation (2.3). When dispersion is neglected, this steepening leads to a gradient catastrophe, the formation of an infinite temporal gradient. This occurs at the finite normalized distance $\zeta_b = 1/max[f_0'(\tau)]$ [2], as well known from the Hopf equation [Eq. (2.6) with $\varepsilon^2 = 0$]. In real-world units the initial value (3.1) develops the gradient catastrophe at distance $z_b = 1.299 L_{nl}$. However, this must be taken as a rough estimate, because, in the presence of dispersion, the actual catastrophe never occurs and oscillations start to appear before such distance [19], owing to the regularizing mechanism which allows for the formation of DSWs.

In this paper we present the results of three data sets whose nominal parameters at the wave maker are reported in Table 1. We also report the estimated dispersive and nonlinear length scales, as well as the ε^2 parameter and the Ursell number. Without loss of generality, we have chosen the characteristic time scale of the initial condition as t_0 in Eq. (3.1). Note that the three runs (henceforth labeled as A, B, C) are characterized by different Ursell number or equivalently different dispersion smallness (parameter ε^2). However, this is not the only parameter that determines the prominence of the DSW. Indeed, working in a tank of finite length, the nonlinear length is also crucial since it affects the length scale over which the DSW develops. From this point of view, it is interesting to note that the last case (run C) has, in spite of intermediate value of ε^2, a much shorter nonlinear length L_{nl}, which allows us to envisage the appearance of the dispersive undulations right in front of the wave maker.

In Fig. 2 we show four time series of the surface elevation measured at different distances from the wave maker, exhibiting the evolution of the dispersive shock along the tank for run A. Note that the last displayed data is taken at 65 meters from the wave maker [see Fig. 2(d)]. Indeed, even though a measurement of the surface elevation is also available at 75 meters, such data start to become visibly affected by the reflection from the beach and will not be presented herein (in particular the residual reflection from the leading edge, that exhibits a strong jump from negative to positive elevations and arrives first at the beach, limits the resolution of the small oscillations in the trailing edge of the DSW, that arrives later). This run is characterized by a relatively small initial amplitude which results into a relatively weak nonlinearity. Nevertheless, even at such small amplitude the nonlinearity is considerably stronger than dispersion, since the nondimensional dispersive parameter turns out to be $\varepsilon^2 \simeq 0.056$, while the measurement range of 75 meters amounts to nearly twice the nonlinear length scale. At 5 meters from the wave maker no oscillations are visible. However, one can clearly recognise the steepening of the positive slope edge of the initial shape, as opposed to the smoothing of the negative slope edge. The oscillations start to become visible at 25 meters (before the distance $z_b \sim 40$ meters estimated from the dispersionless limit) and becomes more pronounced at 45 meters, whereas at 65 meters we can clearly count as many as 6 oscillations of decreasing amplitude towards the trailing edge.

In Fig. 3 we present the case of run B, where the initial amplitude is just doubled with respect to the previous case, without changing the duration. This results into the smallest value of the dispersion parameter ε^2, which now is halved ($\varepsilon^2 \simeq 0.028$), while the nonlinear length scales down to around 16 meters (also the dispersionless estimate for the catastrophe scales down to $z_b \sim 21$ meters). As a consequence the formation of the DSW speeds up. As in previous case strong steepening is observed at 5 meters, while at 25 meters from the wave maker, at least 5 oscillations are clearly observed. At 45 and 65 meters the DSW further expand presenting a very clean structure featuring several oscillations.

The case which displays the most extended region filled with oscillations arising from the regularization of the shock is case C, shown in Fig. 4. This run has been repeated few times with the same excitation conditions to be sure about the full reproducibility of the results. The run is characterized by an excitation with much larger amplitude ($\eta_0 = 10$ cm) and a shorter time scale $t_0 \simeq 0.64$. This results into a slightly higher ratio between the nonlinear and dispersion length scales compared with run B, namely $\varepsilon^2 = 0.045$, which is intermediate between the two previous cases. However, the nonlinear length is much shorter ($L_{nl} \sim 3.4$ m) which allows the DSW to develop over a much shorter length scale. Indeed, well developed oscillations are already observed at the first probe (5 meters from the generator, while the estimate from Hopf equation is $z_b \sim 4$ m), beyond which point the DSW continues to expand, while presenting a quite regular structure over a considerable time span (up to > 50 sec). In this case the DSW presents more than 50 regular oscillations from the leading to the trailing edges and its corresponding spatial extension becomes a considerable fraction of the whole tank (see also the discussion of Fig. 10 in Section 4). On one hand, this further limits to 45 m the maximum distance where the data are not significantly affected by the residual reflection of the leading edge [see Fig. 4(d)]. On the other hand, the recorded data at 35 and 45 meters allows us to clearly appreciate the typical structure of the DSW as a modulated periodic nonlinear wave. A zoom of the undular region of the shock at 35 meters, reported in Fig. 5, shows that the modulation of the amplitude of the oscillations is accompanied by a modulation of the frequency of the wavetrain (or associated wavelength in space), which varies from the value $f \sim 0.55$ Hz over the strongest oscillation at the leading edge, to $f \sim 1.5$ Hz over the small quasi-linear oscillations associated with the trailing edge. This is also consistent with the spectrum of the measured time series, shown in Fig. 5, which shows a peak around $f \sim 0.55$ Hz which broaden considerably towards the higher frequencies. This implies that the nonlinear modulated wave is not monochromatic (as expected), being rather characterized by a slowly varying frequency (wavelength) of its oscillations. These 'higher frequency' tails challenge the use of the standard shallow water models of the KdV type, to model DSWs. In the next Section, the experimental results will be compared to the numerical simulations of Whitham and KdV equations to deepen this point.

4. Numerical simulations and comparison with experimental data

For reasons described before, we have performed numerical simulations of the KdV and Whitham equations in their time-like form, i.e. Eq. (2.3) and Eq. (2.11). A pseudo-spectral treatment of the time dependence together with a leap-frog scheme in the evolution variable has been adopted [63]. Once more, we underline that for large values of kh the linear dispersion relation of equation (2.3) approximates better the full linear dispersion relation with respect to the standard KdV, Eq. (2.1). This is somehow an unexpected result that allows us to push numerically slightly the KdV equation beyond its formal asymptotic validity.

The initial condition at $z = 0$ is nominally provided by Eq. (3.1); however, as mentioned before, the generation of such function in a wave tank is not an easy task, therefore, besides some preliminary numerical simulations performed with the nominal initial condition, we have also performed some simulations using initial conditions taken from the measurement of the surface elevation at the first probe, positioned at 5 meters from the wave maker.

Here, we first present the results of numerical simulations of Eqs. (2.3) and (2.11) obtained by starting from the nominal initial conditions, Eq. (3.1), for run A, see table 1. In Figure 6 we show the surface elevation measured at 5 meters from the wave maker (probe 1) and the outcome of the numerical simulations. As can be seen from figure, already at such a short distance there are some small but evident discrepancies between the numerics and the experiments. At larger distances, see Figure 7, despite the fact that the main oscillations are captured by both

models, such discrepancies are more evident. A priori, it is difficult to establish if the observed deviations are related to some deficiencies of the models to capture the experimental data or to some discrepancies between the nominal and the actual initial condition generated in the tank. Having in mind such possible source of error, we have performed numerical simulations using directly the data from the first probe as initial condition for the numerics. As can be seen in Figure 8, where the surface elevation is plotted at 65 meters from the wave maker (almost 2 nonlinear lengths), a very good agreement between the experimental data and the numerics is achieved. Both T-KdV and T-Whitham perform equally well.

Similar results can be observed for run B, see Fig. 9. In this latter case, both models capture very well the phase and the amplitude of the first waves but clearly the T-Whitham equation is superior to the T-KdV equation in describing the higher frequency waves at the trailing edge of the DSW. This result is mostly due to exactness of the linear dispersion relation of the Whitham equation.

The last comparison that we show is with run C, the one characterized by an intermediate Ursell number but with very short nonlinear space scale ($L_{nl} = 3.4$ m). First, we report in Fig. 10 the results of the numerical integration of the T-KdV equation with the nominal initial elevation with sech^2-shape. In order to show how the shock fan looks like in this case, we show in Fig. 10(a) a color level plot of the evolution in the lab frame, i.e. in the plane (t, z). The different velocities of the leading and trailing edges which define the shock fan (the region filled with undulations) can be clearly seen, though the velocity term proportional to c_0^{-1} in Eq. (2.3) is responsible for the oblique appearance of the fan. While measurements are performed at fixed distances against time and hence corresponds to horizontal cuts of such plot, in order to give an idea of how the DSW would appear in space by looking at the tank at a fixed instant of time, we report a vertical cut of such plot in Fig. 10(b). As shown, when the leading edge depression arrives at the last gauge (75 meters), the DSW extends over more than 40 meters, occupying a significant portion of the tank, consistently with what we have visually observed during the experimental runs.

In Fig. 11 we show a quantitative comparison of the data with the results of the numerical integration performed with the data at gauge 1 as initial data. The comparison is shown at 45 meters, i.e. more than 10 nonlinear lengths from the wave maker. Again the T-Whitham equation describes better the phases of the DSW with respect to the T-KdV. We emphasize that the oscillations over the trailing tail of the DSW have a period in the range 0.7-0.8 s (equivalent to a wavelength of nearly 1 m). Keeping in mind that the water tank has a water depth of 0.4 meters, the shallow water parameter, kh, assumes the value of 2.5, i.e. well beyond the formal validity of the KdV equation. Also the first undulations are characterized by a period that leads to $kh \simeq 0.7$, not exactly the shallow water limit. We believe that such satisfactory agreement observed is related to the fact that the KdV equation written as an evolution equation in space has better linear properties with respect to the standard KdV, as evinced from Fig. 1.

5. Conclusions

In summary, we have investigated the evolution of non-soliton negative initial data propagating in fixed depth (40 cm) shallow water along a tank (sea-basin) with rectangular section. The recorded time series shows clear evidence for the formation of clean DSW structure. These are characterised by the onset of spontaneous oscillations that emerge from the edge of the steepened (positive slope) front of the initial waveform, and expand afterwards. We have presented three significant cases which differ in terms of the initial wave amplitude and duration, thus resulting into different length scales of the nonlinearity and different relative weakness of the dispersive effects. The case characterised by the highest level of nonlinearity exhibits a quite extensive undular structure with regular oscillations in excess of 50 periods after 45 meters of propagation. This has allowed us to clearly identify the underlying structure of the DSW as a modulated nonlinear wave. Indeed, while the amplitude of the oscillations decreases from the leading to the trailing edge of the dispersive shock, the frequency (wavenumber) increases substantially. We believe that such results considerably improve the understanding of undular bore formation in shallow water, and gives important indications for the investigation of the dynamics of dispersive shock waves in general.

In order to compare the experimental data (recorded in time at fixed locations along the tank) with numerical simulations based on model equations which characterise the propagation in shallow water, we have made use of the version of such models which employ the spatial variable as the evolution variable. The KdV equation, formulated in this way, is characterised by a dispersion relationship which better approximates the exact dispersion relationship. This explains why the observed dynamics is reasonably described by the weakly dispersing KdV equation in all the cases discussed. However, as the nonlinearity increases and the shock fan becomes more extended, a more accurate description of the low-amplitude oscillations near the trailing edge can be obtained by employing the nonlocal Whitham equation. This is due to the fact that such equation improves the description for higher frequencies (i.e., relatively short waves), which are indeed characteristic of the trailing edge of DSWs.

Acknowledgments Grant no. PRIN 2012BFNWZ2 from MIUR is gratefully acknowledged. M.O. was also supported by ONR grant no. 214N000141010991. S.T. and M.O. thank Tamara Grava and B. Giulinico for fruitful discussions.

References

[1] M. Hoefer, M. Ablowitz, Dispersive shock waves, Scholarpedia 4 (11) (2009) 5562.
[2] G. B. Whitham, Linear and nonlinear waves, Vol. 42, John Wiley & Sons, 2011.
[3] S. Moiseev, R. Sagdeev, Collisionless shock waves in a plasma in a weak magnetic field, Journal of Nuclear Energy. Part C, Plasma Physics, Accelerators, Thermonuclear Research 5 (1) (1963) 43.
[4] R. Taylor, D. Baker, H. Ikezi, Observation of collisionless electrostatic shocks, Physical Review Letters 24 (5) (1970) 206.

[5] N. J. Zabusky, M. D. Kruskal, Interaction of" solitons" in a collisionless plasma and the recurrence of initial states, Physical review letters 15 (6) (1965) 240.

[6] D. J. Korteweg, G. De Vries, On the change of form of long waves advancing in a rectangular canal, and on a new type of long stationary waves, The London, Edinburgh, and Dublin Philosophical Magazine and Journal of Science 39 (240) (1895) 422–443.

[7] J. Boussinesq, Essai sur la théorie des eaux courantes,Mémoires présentés par divers savants a l'Acad. des Sci. Inst. Nat. France, XXIII, pp. 1-680, 1877, Vol. 2, Imprimerie nationale, 1877.

[8] E. De Jager, On the origin of the korteweg-de vries equation, arXiv preprint math/0602661.

[9] B. Dubrovin, S. Novikov, Periodic and conditionally periodic analogs of the manysoliton solutions of the korteweg-de vries equation, Sov. Phys.-JETP 40 (6) (1975) 1058–1063.

[10] A. Gurevich, L. Pitaevskii, Nonstationary structure of a collisionless shock wave, Zhurnal Eksperimentalnoi i Teoreticheskoi Fiziki 65 (1973) 590–604.

[11] G. Whitham, Non-linear dispersive waves, Proceedings of the Royal Society of London A: Mathematical, Physical and Engineering Sciences 283 (1393) (1965) 238–261.

[12] H. Flaschka, M. Forest, D. McLaughlin, Multiphase averaging and the inverse spectral solution of the kortewegde vries equation, Communications on Pure and Applied Mathematics 33 (6) (1980) 739–784.

[13] P. D. Lax, C. D. Levermore, The small dispersion limit of the korteweg-de vries equation. i, Selected Papers Volume I (2005) 463–500.

[14] P. D. Lax, C. D. Levermore, The small dispersion limit of the korteweg-de vries equation. ii, Communications on pure and applied mathematics 36 (5) (1983) 571–593.

[15] P. D. Lax, C. D. Levermore, The small dispersion limit of the korteweg-de vries equation. iii, Communications on pure and applied mathematics 36 (6) (1983) 809–829.

[16] P. Lax, C. Levermore, S. Venakides, The generation and propagation of oscillations in dispersive initial value problems and their limiting behavior, in: Important developments in soliton theory, Springer, 1993, pp. 205–241.

[17] S. Venakides, The zero dispersion limit of the korteweg-de vries equation for initial potentials with non-trivial reflection coefficient, Communications on Pure and Applied Mathematics 38 (2) (1985) 125–155.

[18] G. El, V. Khodorovsky, Evolution of a solitonless large-scale perturbation in korteweg-de vries hydrodynamics, Physics Letters A 182 (1) (1993) 49 – 52.

[19] T. Grava, C. Klein, Numerical solution of the small dispersion limit of korteweg-de vries and whitham equations, Communications on Pure and Applied Mathematics 60 (11) (2007) 1623–1664.

[20] T. Claeys, T. Grava, Solitonic asymptotics for the korteweg-de vries equation in the small dispersion limit, SIAM Journal on Mathematical Analysis 42 (5) (2010) 2132–2154.

[21] T. Grava, C. Klein, A numerical study of the small dispersion limit of the kdv equations and asymptotic solutions, Physica D 241 (11) (2012) 22–46–2264.

[22] B. Dubrovin, S. Novikov, The hamiltonian formalism of one-dimensional systems of hydrodynamic type and the bogoliubov-whitham averaging method, in: Akademiia Nauk SSSR, Doklady, Vol. 270, 1983, pp. 781–785.

[23] B. A. Dubrovin, S. P. Novikov, Hydrodynamics of weakly deformed soliton lattices. differential geometry and hamiltonian theory, Russian Mathematical Surveys 44 (6) (1989) 35–124.

[24] B. Dubrovin, On hamiltonian perturbations of hyperbolic systems of conservation laws, ii: universality of critical behaviour, Communications in mathematical physics 267 (1) (2006) 117–139.

[25] B. Dubrovin, T. Grava, C. Klein, A. Moro, On critical behaviour in systems of hamiltonian partial differential equations, Journal of Nonlinear Science 25 (3) (2015) 631–707.

[26] Z. Dutton, M. Budde, C. Slowe, L. V. Hau, Observation of quantum shock waves created with ultra-compressed slow light pulses in a bose-einstein condensate, Science 293 (5530) (2001) 663–668.

[27] M. Hoefer, M. Ablowitz, I. Coddington, E. Cornell, P. Engels, V. Schweikhard, Dispersive and classical shock waves in bose-einstein condensates and gas dynamics, Physical Review A 74 (2) (2006) 023623.

[28] J. Chang, P. Engels, M. Hoefer, Formation of dispersive shock waves by merging and splitting bose-einstein condensates, Physical review letters 101 (17) (2008) 170404.

[29] M. Hoefer, P. Engels, J. Chang, Matter–wave interference in bose–einstein condensates: A dispersive hydrodynamic perspective, Physica D: Nonlinear Phenomena 238 (15) (2009) 1311–1320.

[30] R. Meppelink, S. Koller, J. Vogels, P. Van Der Straten, E. Van Ooijen, N. Heckenberg, H. Rubinsztein-Dunlop, S. Haine, M. Davis, Observation of shock waves in a large bose-einstein condensate, Physical Review A 80 (4) (2009) 043606.

[31] J. Joseph, J. E. Thomas, M. Kulkarni, A. G. Abanov, Observation of shock waves in a strongly interacting fermi gas, Physical Review Letters 106 (15) (2011) 150401.

[32] J. E. Rothenberg, D. Grischkowsky, Observation of the formation of an optical intensity shock and wave breaking in the nonlinear propagation of pulses in optical fibers, Physical review letters 62 (5) (1989) 531.

[33] W. Wan, S. Jia, J. W. Fleischer, Dispersive superfluid-like shock waves in nonlinear optics, Nature Physics 3 (1) (2007) 46–51.

[34] N. Ghofraniha, C. Conti, G. Ruocco, S. Trillo, Shocks in nonlocal media, Physical review letters 99 (4) (2007) 043903.

[35] S. Jia, W. Wan, J. W. Fleischer, Dispersive shock waves in nonlinear arrays, Physical review letters 99 (22) (2007) 223901.

[36] C. Conti, A. Fratalocchi, M. Peccianti, G. Ruocco, S. Trillo, Observation of a gradient catastrophe generating solitons, Physical review letters 102 (8) (2009) 083902.

[37] N. Ghofraniha, L. S. Amato, V. Folli, S. Trillo, E. DelRe, C. Conti, Measurement of scaling laws for shock waves in thermal nonlocal media, Optics letters 37 (12) (2012) 2325–2327.

[38] N. Ghofraniha, S. Gentilini, V. Folli, E. DelRe, C. Conti, Shock waves in disordered media, Physical review letters 109 (24) (2012) 243902.

[39] J. Fatome, C. Finot, G. Millot, A. Armaroli, S. Trillo, Observation of optical undular bores in multiple four-wave mixing, Physical Review X 4 (2) (2014) 021022.

[40] A. Kamchatnov, R. A. Kraenkel, B. Umarov, Asymptotic soliton train solutions of the defocusing nonlinear schrödinger equation, Physical Review E 66 (3) (2002) 036609.

[41] A. Fratalocchi, C. Conti, G. Ruocco, S. Trillo, Free-energy transition in a gas of noninteracting nonlinear wave particles, Physical review letters 101 (4) (2008) 044101.

[42] S. Trillo, A. Valiani, Hydrodynamic instability of multiple four-wave mixing, Optics letters 35 (23) (2010) 3967–3969.

[43] A. Moro, S. Trillo, Mechanism of wave breaking from a vacuum point in the defocusing nonlinear schrödinger equation, Physical Review E 89 (2) (2014) 023202.

[44] G. A. El, Resolution of a shock in hyperbolic systems modified by weak dispersion, Chaos: An Interdisciplinary Journal of Nonlinear Science 15 (3) (2005) 037103.

[45] T. B. Benjamin, M. Lighthill, On cnoidal waves and bores, in: Proceedings of the Royal Society of London A: Mathematical, Physical and Engineering Sciences, Vol. 224, The Royal Society, 1954, pp. 448–460.

[46] D. Peregrine, Calculations of the development of an undular bore, Journal of Fluid Mechanics 25 (02) (1966) 321–330.

[47] R. Johnson, Shallow water waves on a viscous fluidthe undular bore, Physics of Fluids (1958-1988) 15 (10) (1972) 1693–1699.

[48] H. Chanson, Tidal Bores, Aegir, Eagre, Mascaret, Pororoca: Theory and Observations, World Scientific, Singapore, 2011.

[49] H. Favre, Etude théorique et expérimentale des ondes de translation dans les canaux découverts, Dunod, 1935.

[50] H.-H. Prüser, W. Zielke, Undular bores (favre waves) in open channels theory and numerical simulation, Journal of Hydraulic Research 32 (3) (1994) 337–354.

[51] A. Treske, Undular bores (favre-waves) in open channels-experimental studies, Journal of Hydraulic Research 32 (3) (1994) 355–370.

[52] N. Zabusky, C. Galvin, Shallow-water waves, the korteweg-devries equation and solitons, Journal of Fluid Mechanics 47 (04) (1971) 811–824.

[53] J. L. Hammack, A note on tsunamis: their generation and propagation in an ocean of uniform depth, Journal of Fluid Mechanics 60 (04) (1973) 769–799.

[54] H. Segur, The korteweg-de vries equation and water waves. solutions of the equation. part 1, Journal of Fluid Mechanics 59 (04) (1973) 721–736.

[55] J. L. Hammack, H. Segur, The korteweg-de vries equation and water waves. part 2. comparison with experiments, Journal of Fluid mechanics

65 (02) (1974) 289–314.
[56] J. L. Hammack, H. Segur, The korteweg-de vries equation and water waves. part 3. oscillatory waves, Journal of Fluid Mechanics 84 (02) (1978) 337–358.
[57] J. L. Hammack, H. Segur, Modelling criteria for long water waves, Journal of Fluid Mechanics 84 (02) (1978) 359–373.
[58] D. Arcas, H. Segur, Seismically generated tsunamis, Philosophical Transactions of the Royal Society of London A: Mathematical, Physical and Engineering Sciences 370 (2012) 1505–1542.
[59] A. Osborne, M. Petti, Numerical inverse-scattering-transform analysis of laboratory-generated surface wave trains, Physical Review E 47 (2) (1993) 1035.
[60] A. Osborne, M. Petti, Laboratory-generated, shallow-water surface waves: Analysis using the periodic, inverse scattering transform, Physics of Fluids 6 (5) (1994) 1727–1744.
[61] F. Ursell, The long-wave paradox in the theory of gravity waves, in: Proc. Camb. Phil. Soc, Vol. 49, Cambridge Univ Press, 1953, pp. 685–694.
[62] G. Whitham, Variational methods and applications to water waves, in: Proceedings of the Royal Society of London A: Mathematical, Physical and Engineering Sciences, Vol. 299, The Royal Society, 1967, pp. 6–25.
[63] B. Fornberg, G. B. Whitham, A numerical and theoretical study of certain nonlinear wave phenomena, Philosophical Transactions of the Royal Society of London A: Mathematical, Physical and Engineering Sciences 289 (1361) (1978) 373–404.
[64] N. Sanford, K. Kodama, J. D. Carter, H. Kalisch, Stability of traveling wave solutions to the whitham equation, Physics Letters A 378 (30) (2014) 2100–2107.
[65] D. Moldabayev, H. Kalisch, D. Dutykh, The whitham equation as a model for surface water waves, Physica D 309 (2015) 99–107.
[66] B. Deconinck, O. Trichtchenko, High-frequency instabilities of small-amplitude solutions of hamiltonian pdes, arXiV (2015) 1505.03688.
[67] G. F. Clauss, The taming of the shrew: Tailoring freak wave sequences for seakeeping tests, Journal of Ship Research 52 (2008) 194–226.
[68] F. Biésel, F. Suquet, Les apparails générateurs de houle en laboratoire, La Houille Blanche 2 (1951) 147–165.

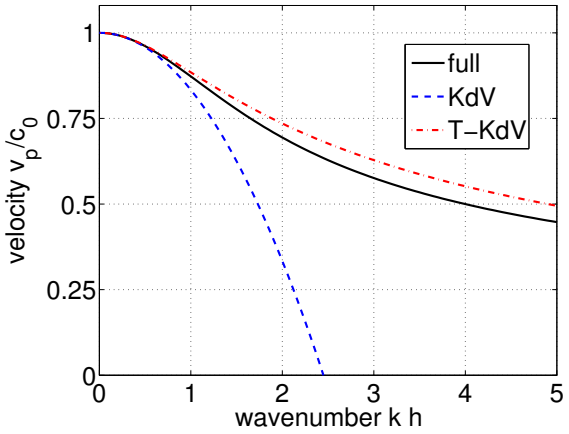

Figure 1. Normalized dispersion relationship, comparing the phase velocity v_p/c_0 as a function of nondimensional wavenumber kh in the full case (solid line), the standard KdV (dashed line), and the T-KdV (dot-dashed line).

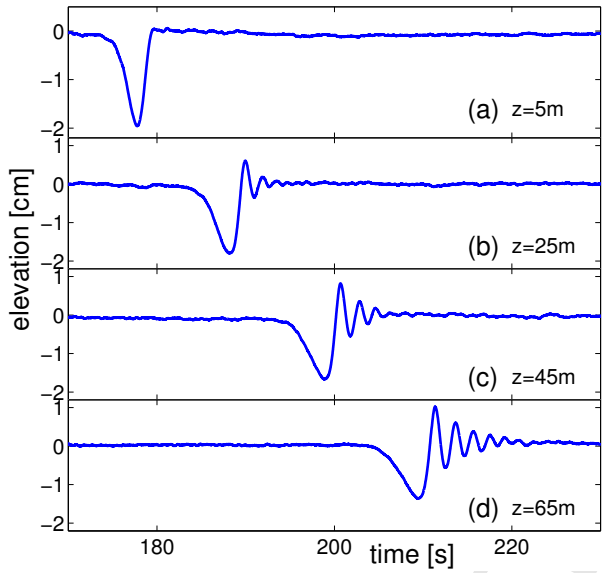

Figure 2. (Color online) Run A - Surface elevation measured at different distances from the wave maker. Nominal initial conditions are characterized by $\eta_0 = 2$ cm and $t_0 = 1.27$ s; see Table 1 for more details.

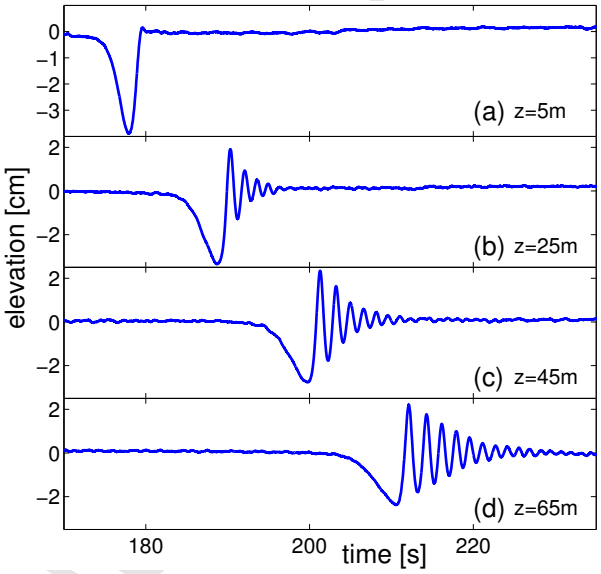

Figure 3. (Color online) Run B - Surface elevation measured at different distances from the wave maker. Nominal initial conditions are characterized by $\eta_0 = 4$ cm and $t_0 = 1.27$ s; See Table 1 for more details.

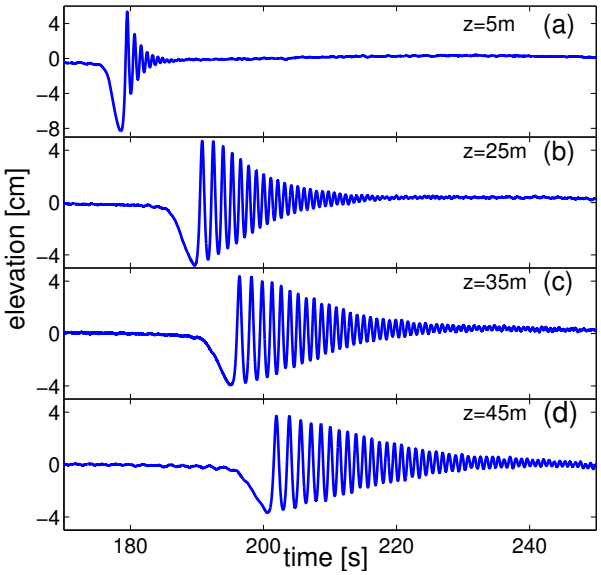

Figure 4. (Color online) Run C - Surface elevation measured at different distances from the wave maker. Nominal initial conditions are characterized by $\eta_0 = 10$ cm and $t_0 = 0.64$ s; See Table 1 for more details.

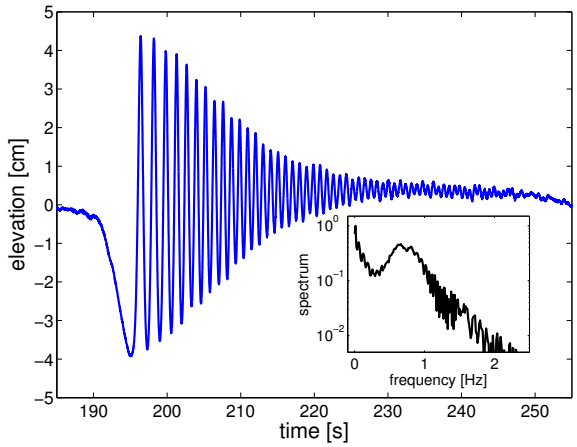

Figure 5. (Color online) Time series of surface elevation measured at z=35 meters for run C. The inset shows its Fourier spectrum: absolute value of the transform (in log units) vs. frequency (only positive frequencies are shown since the spectrum is symmetric).

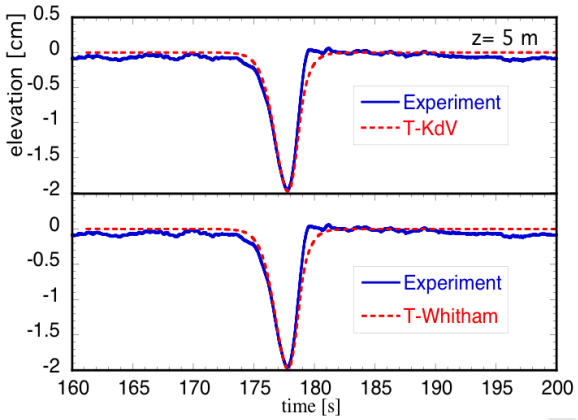

Figure 6. (Color online) Run A - Comparison between the measured surface elevation (solid blue) with numerical computations (dashed in red) of the T-KdV (upper panel) and T-Whitham (lower panel) equations at 5 meters from the wave maker (probe 1). Initial conditions for the simulations are provided by $\eta(z=0,t) = -\eta_0 \mathrm{sech}(t/t_0)^2$ with $t_0 = 1.27$ s and $\eta_0 = 2$ cm.

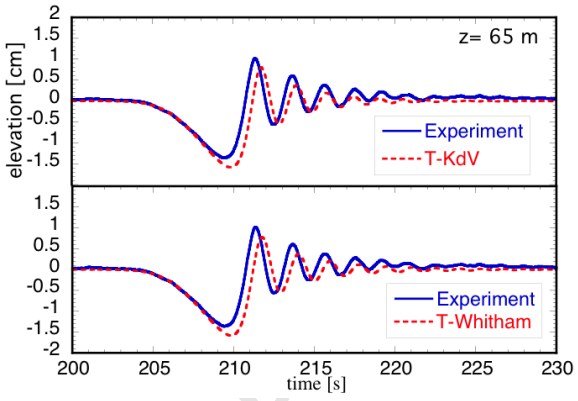

Figure 7. (Color online) Run A - Comparison between the measured surface elevation (solid blue) with numerical computation (dashed in red) of the T-KdV (upper panel) and T-Whitham (lower panel) equations at 65 meters from the wave maker (probe 7). Initial conditions for the simulations are provided by $\eta(z=0,t) = -\eta_0 \mathrm{sech}(t/t_0)^2$ with $t_0 = 1.27$ s and $\eta_0 = 2$ cm.

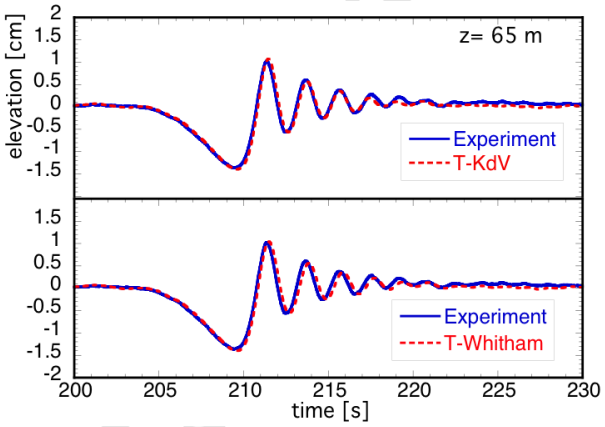

Figure 8. (Color online) Run A - Comparison between the measured surface elevation (solid blue) with numerical computations (dashed in red) of the T-KdV (upper panel) and T-Whitham (lower panel) equations at 65 meters from the wave maker (probe 1). Initial conditions for the simulations are provided by the surface elevation recorded at 5 meters from the wave maker (probe 1).

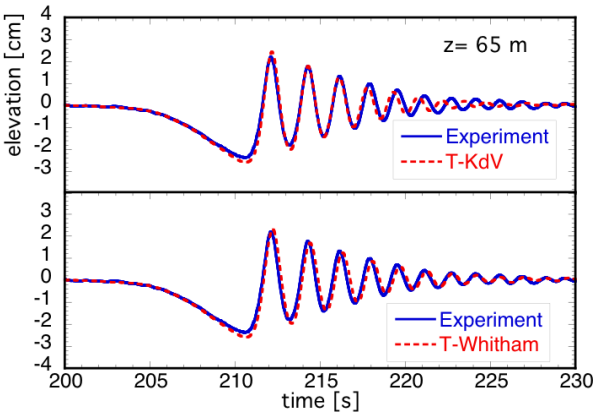

Figure 9. (Color online) Run B - Comparison between the measured surface elevation (solid blue) with numerical computations (dashed in red) of the T-KdV (upper panel) and T-Whitham (lower panel) equations at 65 meters from the wave maker (probe 1). Initial conditions for the simulations are provided by the surface elevation recorded at 5 meters from the wave maker (probe 1).

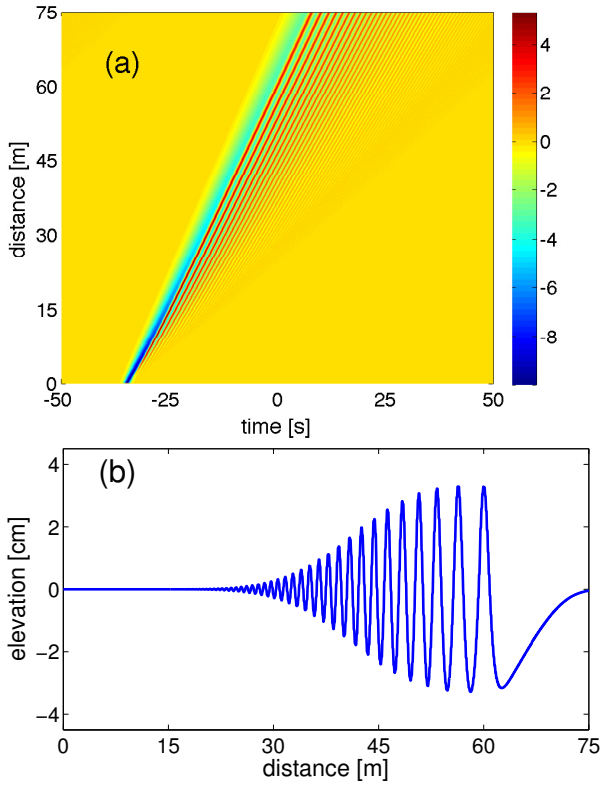

Figure 10. (Color online) Run C - (a) False colorplot of the water elevation (color correspondence to elevation in cm is shown on the right), showing the formation of the characteristic shock fan in the plane (t, z), i.e. in the laboratory frame. (b) Vertical section from panel (a) showing the water elevation vs. distance z along the tank at a fixed time [$t = 0$ in (a); note that the origin of time here does not correspond to the origin of time in the measurements]. The results are obtained from numerical integration of the T-KdV with nominal initial condition $\eta(z = 0, t) = -\eta_0 \mathrm{sech}[(t + 35)/t_0)^2$ with $t_0 = 0.64$ s and $\eta_0 = 10$ cm.

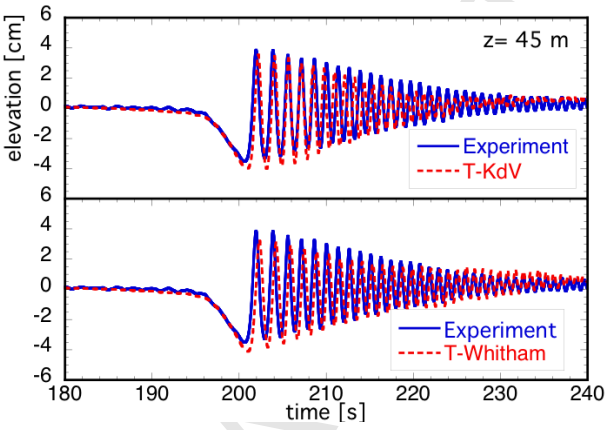

Figure 11. (Color online) Run C - Comparison between the measured surface elevation (solid blue) with numerical computations (dashed in red) of the T-KdV (upper panel) and T-Whitham (lower panel) equations at 45 meters from the wave maker (probe 1). Initial conditions for the simulations are provided by the surface elevation recorded at 5 meters from the wave maker (probe 1).